

# All-optical tunable group-velocity control of femtosecond pulse by quadratic nonlinear cascading interactions

Wenjie Lu<sup>1</sup>, Yuping Chen<sup>1\*</sup>, Lihong Miu<sup>1</sup>, Xianfeng Chen<sup>1\*\*</sup>, Yuxing Xia<sup>1</sup> and Xianglong Zeng<sup>2</sup>

<sup>1</sup> Department of Physics,

State key lab of advanced optical communication systems and networks,  
Shanghai Jiaotong University, 200240, Shanghai, China

<sup>2</sup> Key Laboratory of Special Fiber Optics and Optical Access Networks,  
Shanghai University, 149 Yanchang Road, 200072, Shanghai, China  
[ypchen@sjtu.edu.cn](mailto:ypchen@sjtu.edu.cn), [xfchen@sjtu.edu.cn](mailto:xfchen@sjtu.edu.cn)

**Abstract:** Based on cascading nonlinear interactions of second harmonic generation (SHG) and difference frequency generation (DFG), we present a novel scheme to control the group velocity of femtosecond pulse in MgO doped periodically poled lithium niobate crystal. Group velocity of tunable signal pulse can be controlled by another pump beam within a wide bandwidth of 180nm. Fractional advancement of 2.4 and fractional delay of 4 are obtained in our simulations.

©2008 Optical Society of America

**OCIS codes:** (190.0190) Nonlinear optics; (190.2620) Frequency conversion; (190.7110) Ultrafast nonlinear optics; (320.2250) Femtosecond phenomena

---

## References and links

1. L. Brillouin, *Wave propagation and group velocity* (Academic Press, New York, 1960).
2. R.W. Boyd and D. J. Gauthier, "Slow and fast light," *Progress in Optics* 43, edited by E. Wolf, 497–529, (Elsevier, Amsterdam, 2002).
3. L. V. Hau, S. E. Harris, Z. Dutton, and C. H. Behroozi, "Light speed reduction to 17 metres per second in an ultracold atomic gas," *Nature* **397**, 594–598 (1999).
4. M. S. Bigelow MS, N. N. Lepeshkin, R. W. Boyd, "Superluminal and slow light propagation in a room temperature solid," *Science* **301**, 200–202 (2003).
5. M. D. Stenner, D. J. Gauthier, and M. A. Neifeld, "The speed of information in a 'fast-light' optical medium," *Nature* **425**, 695–698 (2003).
6. M. O. Scully, "Ultraslow group velocity and enhanced nonlinear optical effects in a coherently driven hot atomic gas," *Phys. Rev. Lett.* **82**, 5229–5232 (1999).
7. L. J. Wang, A. Kuzmich, A. Dogariu, "Gain-assisted superluminal light propagation," *Nature* **406**, 277–279 (2000).
8. Yurii A. Vlasov<sup>1</sup>, Martin O'Boyle<sup>1</sup>, Hendrik F. Hamann<sup>1</sup> & Sharee J. McNab, "Active control of slow light on a chip with photonic crystal waveguides," *Nature* **438**, 65–69 (2005).
9. Pei-Cheng Ku, Forrest Sedgwick, Connie J. Chang-Hasnain, Phedon Palinginis, Tao Li, Hailin Wang, Shu-Wei Chang and Shun-Lien Chuang, "Slow light in semiconductor quantum wells," *Opt. Lett.* **29**, 2291–2293 (2004).
10. Yuping Chen, Zhimin Shi, Petros Zerom and Robert W. Boyd, "Slow Light with Gain Induced by Three Photon Effect in Strongly Driven Two-Level Atoms," in *Slow and Fast Light 2006*, Technical Digest (CD) (Optical Society of America, 2006), paper ME1.
11. M. S. Bigelow, N. N. Lepeshkin, R. W. Boyd, "Observation of Ultraslow Light Propagation in a Ruby Crystal at Room Temperature," *Phys. Rev. Lett.* **90**, 113903 (2003).
12. M. S. Bigelow, *Ultra-Slow and Superluminal Light Propagation in Solids at Room Temperature* (PHD thesis, 2004), Chap. 6.
13. George M. Gehring, Aaron Schweinsberg, Christopher Barsi, Natalie Kostinski and Robert W. Boyd, "Observation of Backwards Pulse Propagation Through a Medium with a Negative Group Velocity," *Science* **312**, 895–897 (2006).

14. Y. Okawachi, M.S. Bigelow, J.E. Sharping, Z. Zhu, A. Schweinsberg, D.J. Gauthier, R.W. Boyd, and A.L. Gaeta "Tunable All-Optical Delays via Brillouin Slow Light in an Optical Fiber," *Phys. Rev. Lett.* **94**, 153902 (2005)
15. Z. Zhu, D. J. Gauthier, Y. Okawachi, J. E. Sharping, A. L. Gaeta, R. W. Boyd, and A. E. Willner, "Numerical study of all-optical slow-light delays via stimulated Brillouin scattering in an optical fiber," *J. Opt. Soc. Am. B* **22**, 2378-2384 (2005).
16. K. Y. Song, M. G. Herr´aez, L. Th´evenaz, "Observation of pulse delaying and advancement in optical fibers using stimulated Brillouin scattering," *Opt. Express* **13**, 82–88 (2005).
17. J. E. Sharping, Y. Okawachi, and A. L. Gaeta, "Wide bandwidth slow light using a Raman fiber amplifier," *Opt. Express* **13**, 6092–6098 (2005).
18. D. Dahan and G. Eisenstein, "Tunable all optical delay via slow and fast light propagation in a Raman assisted fiber optical parametric amplifier: a route to all optical buffering," *Opt. Express* **13**, 6234–6249 (2005).
19. M. Marangoni, C. Manzoni, R. Ramponi, G. Cerullo, F. Baronio, C. De Angelis, and K. Kitamura, "Group-velocity control by quadratic nonlinear interactions," *Opt. Lett.* **31**, 534-536 (2006)
20. Yong Wang, Jorge Fonseca-Campos, Chang-Qing Xu, Shiquan Yang, Evgueni A. Ponomarev, and Xiaoyi Bao, "Picosecond-pulse wavelength conversion based on cascaded second-harmonic generation–difference frequency generation in a periodically poled lithium niobate waveguide," *Appl. Opt.* **45**, 5391-5403 (2006).
21. F. Baronio, C. De Angelis, M. Marangoni, C. Manzoni, R. Ramponi, and G. Cerullo, "Spectral shift of femtosecond pulses in nonlinear quadratic PPSLT Crystals," *Opt. Express* **14**, 4774-4779 (2006)
22. D. E. Zelmon, D. L. Small, and D. Jundt, "Infrared corrected Sellmeier coefficients for congruently grown lithium niobate and 5 mol.% magnesium oxide –doped lithium niobate," *J. Opt. Soc. Am. B* **14**, 3319-3322 (1997).
23. G. P. Agrawal, *Nonlinear Fiber Optics*, 2nd ed. (Academic, 1995).
24. S. Ashihara, T. Shimura, K. Kuroda, Nan Ei Yu, S. Kurimura, K. Kitamura, Myoungsik Cha, and Takunori Taira, "Optical pulse compression using cascaded quadratic nonlinearities in periodically poled lithium niobate," *Appl. Phys. Lett.* **84**, 1055-1057 (2004).
25. Daniel J. Gauthier. "Optical communications: Solitons go slow," *Nature Photonics*. **1** 92-93 (2007)

## 1. Introduction

In recent years, great interests have been focused on how to control the propagation velocity of light pulses in different optical materials [1-9]. Controllable slow light can be used in such applications as optical buffering, variable true time delay, and optical information processing. Early slow- and fast-light researches usually use the large normal and abnormal dispersion associated with a resonance of a material system [3,5,7,10]. Among these, there are two representative methods, electromagnetically induced transparency (EIT) [3] and coherent population oscillations (CPO) [11], which usually require a long duration pulse.

Approaches of delaying ultra-short pulses and that compatible with present fiber-optic communication systems are strongly required. For fibers have several advantages including a broad range of operating wavelengths, operation at room temperature and flexible lengths, various methods based on fiber have been intensively studied. Matthew S. Bigelow etc. extended the study of CPO to single-mode erbium-doped silica fiber [12], which can gain the ability to tune the pulse delay continuously from positive to negative by changing the intensity of pump laser [13]. In this approach, the probe pulse is of ms magnitude, and the obtained fractional delay or advancement is usually less than one, which limits its practical application in communication systems.

By using the dispersion associated with a laser-induced amplifying resonance, stimulated Brillouin scattering (SBS) [14,15,16], stimulated Raman scattering (SRS) [17], and Raman assisted parametric process (OPA) [18] have been extensively proposed to control the group velocity of ultra-short pulse in optical fiber communication systems. By SBS, the slow-light resonance can be created at the desired wavelength by tuning the wavelength of the pump, and pulse delay more than 1 signal pulse duration can be obtained. However, it can only delay ps pulse due to its gain bandwidth of GHz. In addition, they may have some inherent limitations such as pulse distortion accompanied with large pulse delay. Besides, the available bandwidth for slow and fast light in Raman assisted OPA is also tens to hundreds of GHz, which also allows the delay of picoseconds pulse. By SRS, femtosecond pulses can be delayed associated with a gain bandwidth of THz. According to our knowledge, it can only realize relatively

small temporal shift less than 1 pulse duration at certain wavelength. These above constraints of different approaches to control group velocity of optical pulse may limit their performance in all-optical communication systems to some extent.

It is noticed that group velocity of femtosecond pulse can also be controlled by SHG quadratic nonlinear interactions under phase mismatch [19]. In this scheme, more than 1 fractional delay has been reported in a widely tunable wavelength range. In this cascading SHG process, in the cycles of up- and down-conversion between fundamental frequency wave (FF) and second harmonic wave (SH), FF pulse can be dragged by the SH pulse, then the group velocity of FF wave can be modulated by itself.

In this paper, we propose a novel scheme to control the group velocity of femtosecond pulse efficiently by cascading second harmonic generation (SHG) and difference frequency generation (DFG) nonlinear interactions. The remarkable advantages of our scheme are i) ultra-short pulse duration of fs pulse can be delayed or advanced, ii) group velocity of input signal can be efficiently controlled by tuning the pump, rather than modulated by the signal itself, so more flexibility can be provided, iii) over a wide wavelength range of 180nm of input signal, iv) large fractional advancement of 2.4 and fractional delay of 4 can be obtained.

## 2. Theoretical model

In our scheme, we consider that pump and signal pulse are incident onto a z-cut, 30-mm long periodically poled MgO:LiNbO<sub>3</sub> (PPMGLN) crystal along x direction (as shown in Fig. 1). During the propagation in the crystal, the pump pulse (central wavelength at  $\omega_p$ ) generates the second harmonic (SH) wave first, and then the converted wave (central frequency at  $\omega_c$ ) can be generated by DFG between the SH pulse (central frequency at  $\omega_{SH}$ ) and signal pulse (central frequency at  $\omega_s$ ). The energy consequently passes from the pump to the SH, and then the signal and the converted wave back and forth. As a result, the signal decelerates (or accelerates) when it is dragged by the slower (or faster) SH pulse because of the slight group-velocity mismatch (GVM) and energy exchange between signal and SH.

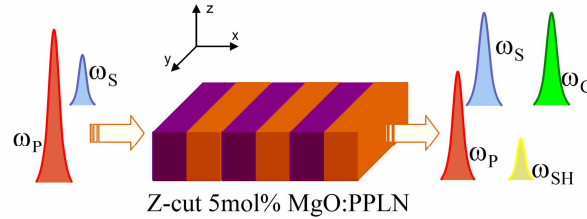


Fig. 1 Schematic of the SHG-DFG cascading process in periodically poled MgO doped lithium niobate crystal

We consider a type I QPM geometry in this quadratic cascading interaction and the nonlinear coefficient  $d_{31}$  is used. The wave-vector mismatching between the pump and the signal (or the converted) is quite large since the central wavelength of the pump is very close to that of the signal (or the converted) in our model, so the very weak direct interaction between the pump wave and the signal (or the converted) can be ignored in our model. Then we just concentrate on these two processes: interaction between the pump and SH wave, interactions among the SH, the signal and the converted waves. Similar to the previous analyses [20, 21], we derive the following coupled mode equations to describe the interactions among the pump, SH, the signal and the converted waves inside the crystal:

$$\frac{\partial A_p}{\partial z} = -\delta^p \frac{\partial A_p}{\partial t} - \frac{j}{2} \beta_2^p \frac{\partial^2 A_p}{\partial t^2} - j\omega_p \kappa_{pp}^* A_p^* A_{SH} \exp(-j\Delta k_p z) - \frac{\alpha_p}{2} A_p \quad (1)$$

$$\begin{aligned} \frac{\partial A_{SH}}{\partial z} = & -\delta^{SH} \frac{\partial A_{SH}}{\partial t} - \frac{j}{2} \beta_2^{SH} \frac{\partial^2 A_{SH}}{\partial t^2} - j\omega_p \kappa_{pp}^* A_p^* A_p \exp(j\Delta k_p z) \\ & - 2j\omega_p \kappa_{sc}^* A_s A_c \exp(j\Delta k_c z) - \frac{\alpha_{SH}}{2} A_{SH} \end{aligned} \quad (2)$$

$$\frac{\partial A_s}{\partial z} = -\frac{j}{2}\beta_2^s \frac{\partial^2 A_s}{\partial t^2} - j\omega_s \kappa_{sc} A_c^* A_{SH} \exp(-j\Delta k_c z) - \frac{\alpha_s}{2} A_s \quad (3)$$

$$\frac{\partial A_c}{\partial z} = -\delta^c \frac{\partial A_c}{\partial t} - \frac{j}{2}\beta_2^c \frac{\partial^2 A_c}{\partial t^2} - j\omega_c \kappa_{sc} A_s^* A_{SH} \exp(-j\Delta k_c z) - \frac{\alpha_c}{2} A_c \quad (4)$$

where  $A_p$ ,  $A_{SH}$ ,  $A_s$ , and  $A_c$ , as functions of the time  $t$  and position  $z$ , represent the complex electric fields of the pump, the SH, the signal, and the converted waves under the slowly varying envelope approximation.  $\beta_1^p$  and  $\beta_2^p$ ,  $\beta_1^{SH}$  and  $\beta_2^{SH}$ ,  $\beta_1^s$  and  $\beta_2^s$ ,  $\beta_1^c$  and  $\beta_2^c$  are the first and second derivatives of the propagation constants with respect to the angular frequency  $\omega$ , which are centered at  $\omega_p$ ,  $\omega_{SH}$ ,  $\omega_s$  and  $\omega_c$  respectively.  $\kappa_{pp}$  and  $\kappa_{sc}$  refer to the SH and the converted wave coupling coefficient.  $\alpha_p$ ,  $\alpha_s$ ,  $\alpha_c$ ,  $\alpha_{SH}$  are the attenuation coefficients for the pump, the SH, the signal, and the converted waves, respectively. We introduce a new time variable  $T=t-z\beta_1^s$  measured in the reference frame moving with the input signal pulse. Thus  $\delta^p=\beta_1^p-\beta_1^s$ ,  $\delta^{SH}=\beta_1^{SH}-\beta_1^s$  and  $\delta^c=\beta_1^c-\beta_1^s$  represent the group-velocity mismatch (GVM) between the signal and pump, the signal and SH, and the signal and the converted. Positive GVM, i.e.  $\delta^i>0$  ( $i=p, SH, c$ ) corresponds to slowing down the signal, and negative GVM means acceleration of the signal.  $\Delta k_p$  and  $\Delta k_c$  represent the phase mismatching in the cascading SHG and DFG processes as follows:

$$\Delta k_p = \beta(\omega_{SH}) - 2\beta(\omega_p) - \frac{2\pi}{\Lambda} \quad (5)$$

$$\Delta k_c = \beta(\omega_{SH}) - \beta(\omega_s) - \beta(\omega_c) - \frac{2\pi}{\Lambda} \quad (6)$$

and

$$\kappa_{pp} = \frac{\sqrt{2\mu_0/cd_{eff}}}{\sqrt{n(\lambda_{SH})n(\lambda_p)^2 A_{eff}}}, \quad \kappa_{sc} = \frac{\sqrt{2\mu_0/cd_{eff}}}{\sqrt{n(\lambda_{SH})n(\lambda_s)n(\lambda_c) A_{eff}}}, \quad d_{eff} = \frac{2}{\pi} d_{31} \quad (7)$$

where  $\Lambda$  is the poling period of PPMGLN crystal.  $\beta$  is the propagation constant with respect to angular frequency.  $\mu_0$  is the permeability of free space, and  $c$  is the light velocity in vacuum.  $\lambda_p$ ,  $\lambda_{SH}$ ,  $\lambda_s$ , and  $\lambda_c$  are the central wavelengths of the pump, SH, the signal and the converted waves respectively.  $d_{eff}$  is the effective nonlinear coefficient, and  $A_{eff}$  is the effective interaction area.  $n$  is the refractive index of the crystal, whose dependence on wavelength can be approximated by the Sellmeier equation of MgO doped LiNbO<sub>3</sub> [22].

### 3. Simulation results

We use the split-step Fourier method [23] to simulate the evolution of the pulses inside the crystal, since the coupled-mode differential equations above can't be solved analytically. For practical consideration, we set the temperature at 25°C in our simulations. In addition, we take  $\alpha_p=\alpha_s=\alpha_c=\alpha_{SH}=0$  dB/cm for simplicity. The length of crystal is 30 mm and  $A_{eff}=45\mu\text{m}^2$ ,  $d_{eff}=16.5\text{pm/V}$ .

Fig 2 shows that the fractional time delay of the signal pulse is 1.5 (120fs/80fs). The pulse width decreases from 80fs to 38fs. This kind of compression of the pulse is due to the nonlinear phase shift induced by the quadratic cascaded interaction, which is similar to the soliton compression mentioned in Ref. [24].

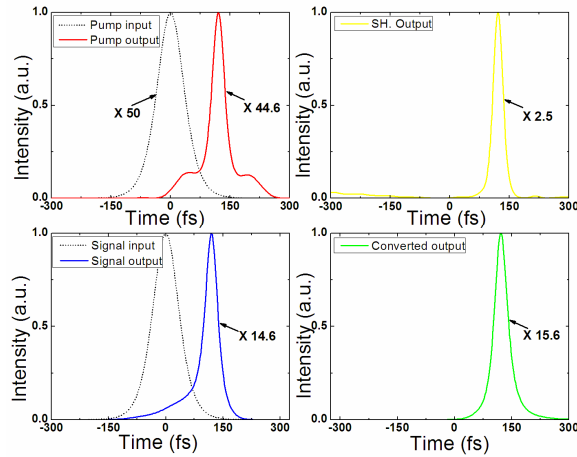


Fig. 2. Normalized pulse intensity of the interaction pulses. Dotted line (solid line) represents the input (output) pulse intensity. The central wavelength of the input pump (signal) pulse is 1550nm (1600nm) with the intensity of 50GW/cm<sup>2</sup> (1GW/cm<sup>2</sup>). The group velocity mismatching between SH and the signal is 9.7227fs/mm, and the corresponding phase mismatching are  $\Delta k_p L = 101.5\pi$  and  $\Delta k_c L = 100\pi$ . Both widths of two pulses durations (FWHM) are 80fs. It can be seen that output signal pulse has been delayed for 120fs with the pulse of 38fs.

By changing the intensity of the pump, or tuning the wavelength of the signal, large delay or advancement of signal pulse is obtained in Fig. 3. We choose the central wavelength of the pump at 1490nm and the signal at 1560nm, which corresponds to the situation of GVM=44.80fs/mm. By decreasing the pump intensity to 0.1 GW/cm<sup>2</sup>, no delay is obtained as the green line shows in Fig. 3, in the meantime, pulse duration broadens to 150 fs due to GVD effect.

By tuning the central wavelength of the pump and the signal to make the sign of the GVM negative (GVM=-5.90fs/mm), we can reach the result of the signal acceleration case as red line shows.

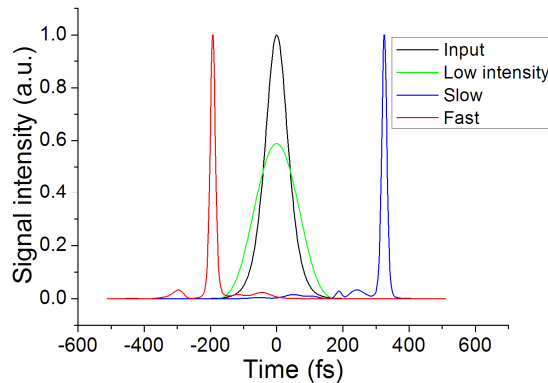


Fig. 3 Demonstration of the group velocity control by changing pump intensity. The black curve is the input pulse and the green (blue and red) curve is the output intensity with input pump intensity at 0.1 GW/cm<sup>2</sup> (100 GW/cm<sup>2</sup>). The red line refers to the advancement case due to negative GVM. The width (FWHM) of red, blue and green pulses is 18fs, 18fs and 150fs and the corresponding delay is -194fs, 326fs and 0fs respectively.

Above results are simulated under the phase mismatching condition of  $\Delta k_p L = 53.95\pi$  and  $\Delta k_c L = 50\pi$ . From Fig.3, it can be seen that both considerable advancement of 194fs and delay of 326fs are obtained.

To study the relation between pump intensity and pulse delay, we set the intensity of input signal pulse at  $1 \text{ GW/cm}^2$  and vary the pump intensity from  $1 \text{ GW/cm}^2$  to  $50 \text{ GW/cm}^2$ . The corresponding time delay and wavelengths (pump and signal) in each of these cases are shown in Fig.4:

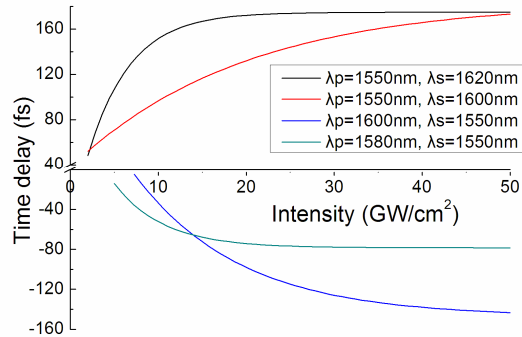


Fig. 4. Time delay of the output signal as a function of the pump input peak intensity. The red and black lines represent the small ( $9.7227 \text{ fs/mm}$ ) and large ( $11.064 \text{ fs/mm}$ ) positive GVM, and the blue and green lines show the negative GVM of  $-22.188 \text{ fs/mm}$  and  $-11.364 \text{ fs/mm}$ . Fractional time delay (advancement) over unit (i.e. time delay more than  $80 \text{ fs}$ ) can be achieved when input pump intensity is larger than  $10 \text{ GW/cm}^2$  ( $20 \text{ GW/cm}^2$ ). The phase matching conditions above are  $\Delta k_p L = 101.31\pi$  and  $\Delta k_s L = 100\pi$

Fig. 4 shows that time delay becomes larger by increasing pump intensity, so that it's possible to control the group velocity of the signal pulse by tuning the intensity of the pump. It also shows that with the same input intensity, different time delay can be obtained with different GVM. It should be noticed that under the large phase mismatching condition, time delay will decrease significantly with the same input pump intensity due to fewer energy exchange between SH and the signal pulse. Besides, tunable time delay or advancement of signal pulse can also be expected by changing phase matching temperature, i.e. changing GVM. Thus, it's more efficient and flexible to control the time delay in our scheme by modulating the intensity of the pump, or tuning its central wavelength, or just changing the temperature of the crystal.

For practical requirement, the bandwidth of delayed signal pulse also needs to be considered seriously. In Fig. 5, we fix the central wavelength of pump at  $1550 \text{ nm}$  and change the signal from  $1460 \text{ nm}$  to  $1640 \text{ nm}$  to see the corresponding time delay. In our calculations, the domain conversion period  $\Lambda$  is  $19.60 \mu\text{m}$ , and the intensity of the input pump (signal) pulse is  $50 \text{ GW/cm}^2$  ( $1 \text{ GW/cm}^2$ ). The durations of both pulses are  $80 \text{ fs}$ .

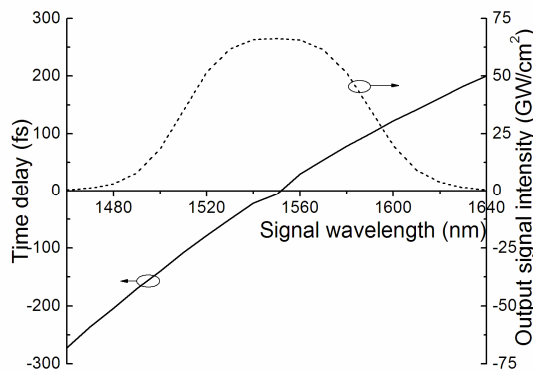


Fig 5. Time delay and output signal intensity as a function of input signal wavelength. Solid line is time delay with different input signal wavelength and dashed line is the corresponding output intensity.

As shown in Fig 5, zero delay of signal pulse can be obtained at 1550nm. When the signal wavelength deviates from 1550nm, the time delay (or advancement) also increases with the intensity decreasing of output signal. When the intensity of the output delayed pulse is much less than that of the input pulse, this kind of delay becomes meaningless. So we define the wavelength range as the effective signal bandwidth when the intensity of the output delayed pulse is more than that of the input signal pulse ( $1\text{GW}/\text{cm}^2$ ). In our simulation, the wavelength bandwidths of delayed and advanced signal are both as large as 90nm.

#### **4. Conclusion**

In summary, we have demonstrated all optical tunable control of femtosecond laser pulse theoretically through SHG and DFG quadratic nonlinear cascading interactions. In our scheme, one of the significant advantages is that we can control the group velocity of the signal pulse by varying the pump intensity within a wide range from  $1\text{GW}/\text{cm}^2$  to  $50\text{GW}/\text{cm}^2$  or even higher. This may help us to find a different practical way to achieve controllable delay lines which are essential in all optical communications. Since the delayed pulse has the soliton feature, this scheme would provide an approach to form the slow light soliton [25].

#### **Acknowledgments**

This research is supported by the National Natural Science Foundation of China (No. 60407006, No. 10574092 and No. 10704047), the National High Technology Research and Development Program (863) of China (No. 2007AA01Z273), the National High Technology Research and Development Program (973) of China (No. 2006CB806000), and the Shanghai Leading Academic Discipline Project (No. B201).